arXiv:2310.19102v2 [cs.LG] 7 Nov 2023

ATOM: LOW-BIT QUANTIZATION FOR EFFICIENT AND ACCURATE LLM SERVING

Yilong Zhao [1 2 *] **Chien-Yu Lin** [2] **Kan Zhu** [2] **Zihao Ye** [2] **Lequn Chen** [2] **Size Zheng** [2 3 *] **Luis Ceze** [2]
Arvind Krishnamurthy [2] **Tianqi Chen** [4] **Baris Kasikci** [2]

ABSTRACT

The growing demand for Large Language Models (LLMs) in applications such as content generation, intelligent chatbots, and sentiment analysis poses considerable challenges for LLM service providers. To efficiently use GPU resources and boost throughput, batching multiple requests has emerged as a popular paradigm; to further speed up batching, LLM quantization techniques reduce memory consumption and increase computing capacity. However, prevalent quantization schemes (e.g., 8-bit weight-activation quantization) cannot fully leverage the capabilities of modern GPUs, such as 4-bit integer operators, resulting in sub-optimal performance.

To maximize LLMs' serving throughput, we introduce Atom, a low-bit quantization method that achieves high throughput improvements with negligible accuracy loss. Atom significantly boosts serving throughput by using low-bit operators and considerably reduces memory consumption via low-bit quantization. It attains high accuracy by applying a novel mixed-precision and fine-grained quantization process. We evaluate Atom on 4-bit weight-activation quantization setups in the serving context. Atom improves end-to-end throughput by up to 7.73× compared to the FP16 and by 2.53× compared to INT8 quantization, while maintaining the same latency target. Code will be released at: https://github.com/efeslab/Atom.

1 INTRODUCTION

Large Language Models (LLMs) are being increasingly integrated into our work routines and daily lives, where we use them for summarization, code completion, and decision-making. Studies report that ChatGPT has over 100 million users, with more than 1 billion website accesses per month (Duarte, 2023). Furthermore, the size and capabilities of LLMs continue to grow to accommodate a broader range of tasks. The high inference demand and model complexity have significantly increased the operational costs, i.e., compute/memory and energy, for LLM service providers to near $1 million daily (Elimian, 2023).

Unsurprisingly, optimizing LLM serving is becoming a pressing concern. Most efforts have focused on improving LLM serving throughput, which is typically achieved by batching requests from various users (Yu et al., 2022; Chen, 2023a; Kwon et al., 2023). Batching multiple requests increases compute intensity and amortizes the cost of loading weight matrices, thereby improving throughput. To further improve batching efficiency, prior work has explored LLM quantization techniques. These techniques employ smaller data types to replace 16-bit floating point (FP16) values, thereby reducing memory consumption and accelerating computation (Lin et al., 2023; Xiao et al., 2023).

However, current quantization schemes do not leverage the full extent of capabilities provided by emerging efficient low-bit hardware support (e.g. Nvidia Ampere (Abdelkhalik et al., 2022) and Qualcomm Hexagon (Wikipedia contributors, 2023)). For instance, several prior approaches have explored weight-only quantization (Lin et al., 2023; Frantar et al., 2023). In these quantization schemes, weights are quantized to an integer representation (e.g., INT3), whereas activations remain in a floating point representation (e.g., FP16). Consequently, weights must be dequantized to the appropriate floating point representation (e.g., FP16) before being multiplied with activations. Therefore, even though weight-only quantization reduces memory consumption, it still requires costly floating-point arithmetic, which is inefficient, especially for large batch sizes.

Another prominent quantization scheme is weight-activation quantization, where both weights and activations are quantized to lower-bit representations. In this scheme,

[*]Work done during the internship at UW. [1]Department of Computer Science and Engineering, Shanghai Jiao Tong University, Shanghai, China [2]School of Computer Science & Engineering, University of Washington, Seattle, United States [3]School of Computer Science, Peking University, Beijing, China [4]School of Computer Science, Carnegie Mellon University, Pittsburgh, United States. Correspondence to: Yilong Zhao <zhaoyilong217@sjtu.edu.cn>, Baris Kasikci <baris@cs.washington.edu>.

Preprint, under review.

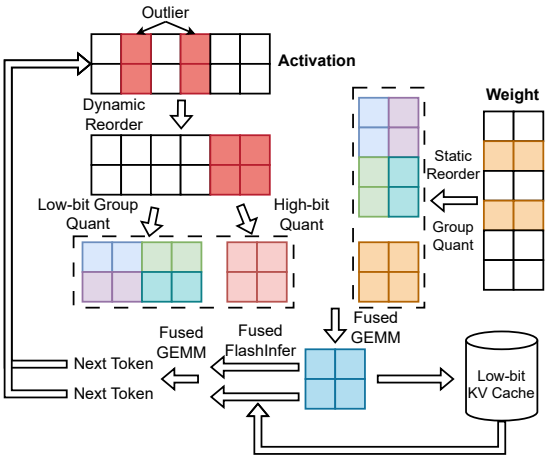

Figure 1. Overview of the Atom quantization design. For activation matrices, we dynamically reorder the channels to pick out the outliers. Then, we apply low-bit group quantization to the normal values while using high-bit precision for outliers. For weight matrices, the quantization process can be done statically. We perform fused GEMM and fused FlashInfer (Ye, 2023) to boost throughput. We also use a quantized KV cache to reduce memory movement.

weights and activations can be directly multiplied using low-precision arithmetic units. This approach has greater potential to achieve higher throughput than weight-only quantization due to the efficient low-bit hardware support. For example, A100 GPUs can reach 1,248 TOPS of INT4 and 624 TOPS of INT8 as opposed to 312 TFLOPS for FP16 (NVIDIA, a). Prior works such as LLM.int8() (Dettmers et al., 2022) and SmoothQuant (Xiao et al., 2023) explored INT8 weight-activation quantization and achieved near no accuracy loss. However, INT8 quantization still cannot utilize lower bit arithmetic such as INT4 TensorCore (NVIDIA, b). In addition, INT8 quantization remains sub-optimal for reducing the large memory consumption in LLM serving, where both model parameters and batched KV-cache consume large memory (Sheng et al., 2023). For lower-bit weight-activation quantization, recent works such as OmniQuant (Shao et al., 2023) and QLLM (Liu et al., 2023a) have proposed to quantize LLMs down to 4-bit. However, their techniques still show a perplexity increase compared to the FP16 baseline as shown in Figure 2. Therefore, determining how to accurately quantize LLMs into low-bit representations while maintaining hardware efficiency remains an open area of research.

In this work, we introduce Atom, an accurate low-bit weight-activation quantization for LLMs that efficiently use modern hardware. To maintain accuracy, Atom incorporates three key quantization designs: (1) It adopts mixed-precision quantization and retains a small but salient number of activations and weights in high precision to preserve accuracy. (2) It employs fine-grained group quantization on both weights and activations, which naturally reduces quantization errors.

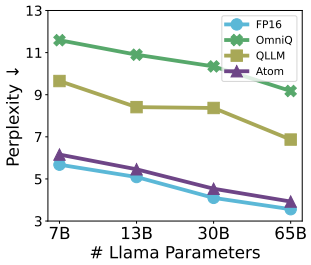

Figure 2. WikiText2 perplexity on the Llama with 4-bit weight-activation quantization (Lower is better). Atom in W4A4 maintains a perplexity close to the FP16 baseline across all model sizes, outperforming existing works.

(3) Instead of pre-calculating quantization parameters for activations, Atom dynamically quantizes activations to best capture the distribution of each input.

Although these quantization optimizations can improve quantization accuracy, they may not use the underlying hardware efficiently without a bespoke design. For example, the mixed-precision technique could lead to irregular memory accesses and performance slowdown (Guo et al., 2023); multiplications with group quantization are not supported in any vendors' library; and dynamic quantization of activations incurs extra computation. To ensure high hardware efficiency and minimize quantization overheads, Atom: (1) reorders activations and weights to maintain regular memory accesses for mixed-precision operations, (2) fuses quantization and reordering operations into existing operators to amortize the overheads, (3) further quantizes outliers into INT8 to keep a balance between accuracy and efficiency and (4) quantizes KV-cache into low-bit to enhance throughput. We illustrate Atom's quantization flow in Figure 1.

To validate Atom's feasibility, we integrate it into an end-to-end serving framework (Chen, 2023b). For our special matrix multiplications with mixed-precision and group quantization, we implement customized CUDA kernels that utilize low-bit tensor cores. Experiments on popular datasets show that Atom has negligible accuracy loss (1.6% average zero-shot accuracy drop, 0.5 perplexity increase for Llama-7B WikiText2) when quantizing Llama (Touvron et al., 2023) models to W4A4 (4-bit for both weights and activations), while prior works suffer larger accuracy loss under the same precision (see Figure 2).

When comparing end-to-end serving throughput to different precisions and quantization schemes, Atom improves throughput by up to 7.7x, 5.5x, and 2.5x relative to FP16, W4A16, and W8A8, respectively, while achieving similar latency (see Figure 11). These results show that Atom can accurately quantize LLMs into very low-precision while achieving high serving throughput.

In summary, we contribute the following:

- An analysis of LLM serving that pinpoints the performance benefit of low-bit weight-activation quantization.
- Atom, an accurate low-bit weight-activation quantization algorithm that combines (1) mixed-precision, (2) fine-grained group quantization, (3) dynamic activation quantization to minimize quantization errors, and (4) KV-cache quantization.
- An integrated LLM serving framework for which we codesign an efficient inference system, implement low-bit GPU kernels, and demonstrate realistic end-to-end throughput and latency of Atom.
- A comprehensive evaluation of Atom, which shows that it improves LLM serving throughput by up to 7.7x with only negligible loss of accuracy.

2 BACKGROUND

Quantization techniques use discrete low-bit values to approximate high-precision floating points. Since integers represent a uniform range, quantizing floating point values into integers is widespread due to simplicity and hardware efficiency (Jacob et al., 2017). Quantization involves two steps: determining the quantization parameters (which consist of scale and zero point) and calculating the quantized tensor. For uniform asymmetric quantization, the scale s and zero point z are determined by (Nagel et al., 2021):

$$s = \frac{\max(X) - \min(X)}{2^n - 1} \times c, z = \lfloor \frac{-\min(X)}{s} \rceil, \quad (1)$$

where X is the input tensor, n is the quantization bit-width, and c is the clipping factor used to reduce the dynamic range of quantization to mitigate the effect of outlier values. The elements in quantized tensor can be calculated by:

$$\bar{X} = \text{clamp}(\lfloor \frac{X}{s} \rceil + z, 0, 2^n - 1).$$

We can further simplify this equation for symmetric quantization:

$$s = \frac{2 \times \max(|X|)}{2^n - 1} \times c$$

$$\bar{X} = \text{clamp}(\lfloor \frac{X}{s} \rceil, -2^{n-1}, 2^{n-1} - 1).$$

Quantization parameters s and z can be calculated either statically using calibration data or dynamically during inference time. Thus, quantization approaches can be classified as static or dynamic.

For LLMs, we can apply quantization on both activation and weight matrices (weight-activation quantization) or just the latter (weight-only quantization). However, asymmetric weight-activation quantization can lead to additional calculations during matrix multiplication since:

$$W \cdot X = s_W(\bar{W} - z_W) \cdot s_x(\bar{X} - z_x),$$

where three additional cross-terms will be calculated. Therefore, we apply symmetric uniform quantization in this work.

We can also apply quantization under different granularity. For **per-tensor** quantization, all the values in the tensor share one set of scale and zero-point. For **per-channel** quantization, we calculate scale and zero-point for a row or a column of the tensor. We can further divide every channel into several groups, and perform quantization on each group, which is **per-group** quantization.

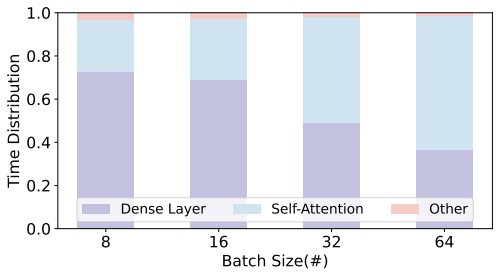

Figure 3. Runtime breakdown of Llama-7b serving with different batch sizes. The dense layer represents the batched K, Q, V generation, O projection, and MLP. The self-attention layer is the batched version of FlashInfer integrated with PageAttention (Kwon et al., 2023). Results indicate that the dense and self-attention layers together account for over 90% of the execution time, thereby constraining the throughput.

3 PERFORMANCE ANALYSIS OF LOW-BIT LLM SERVING

In this section, we first analyze the performance bottleneck of LLM serving and then establish the importance of low-bit weight-activation quantization.

Due to high demand, LLM serving is throughput-oriented. However, the decode stage of LLM inference only takes one token as input and generates the next token, thus relying on matrix-vector multiplication (GEMV). Since GEMV needs to load a large weight matrix while only performing a few multiplications, it is heavily memory-bound. It thus causes GPU under-utilization, which results in low compute intensity (computation-to-IO ratio) and, thereby, low throughput. To mitigate this problem, batching is widely used by combining the input from multiple requests to perform dense layer (K,Q,V generation, O projection, and MLP) matrix multiplications and increase compute intensity and GPU utilization (Pope et al., 2022; Yu et al., 2022; Sheng et al., 2023; Chen, 2023a).

To further boost throughput, the input matrices of the dense

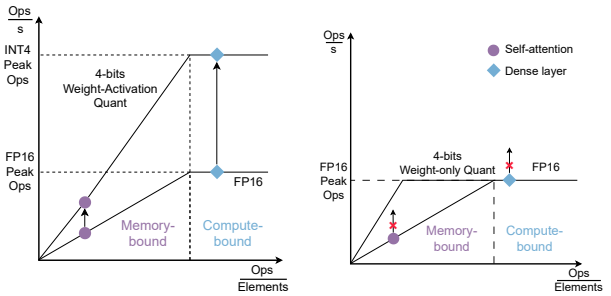

(a) Weight-activation quantization (b) Weight-only quantization.

Figure 4. A roofline model of different quantization approaches that characterizes operators by their arithmetic intensity, which is defined as Ops/Elements. At large batch sizes, the dense layer is compute-bound, which has a large arithmetic intensity, whereas the self-attention exhibits a lower arithmetic intensity.

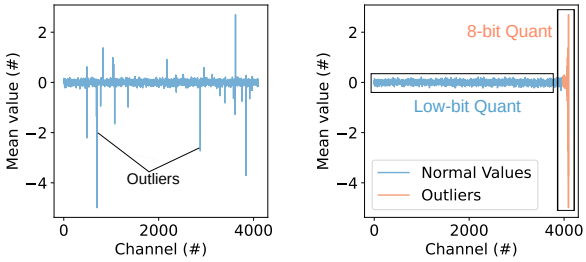

(a) Activation mean values per channel. (b) Mean values after reordering.

Figure 5. The sampled value of the activation matrix. (a) The activation matrix contains outlier channels, which result in large quantization errors. (b) We reorder these outlier channels to the end of the matrix and use higher precision to quantize them while keeping regular memory access.

layer of the decode and prefill stages are batched to form larger matrices, which further amortizes the memory movement of the weight matrix and exploits the batching effect. Given large batch sizes, the dense layer becomes compute-bound. However, although self-attention layers in the decode stage are also GEMV operations, inference requests do not share the KV-cache. Therefore, self-attention layers cannot be batched and need to be performed sequentially. The self-attention layers are still bounded by large memory movement due to KV-cache, even with highly-optimized kernels (e.g. FlashAttention (Dao, 2023)).

After applying the batching technique, we measure the time breakdown of different operators under different batch sizes. As Figure 3 shows, both the dense and self-attention layers act as bottlenecks to throughput, consuming over 90% of the processing time. Consequently, we employ quantization mechanisms to expedite the dense and self-attention layers.

We use the Roofline model (Williams et al., 2009) to evaluate the effect of quantization approaches. As Figure 4(a) shows, weight-activation quantization has higher dense layer compute throughput due to the efficient low-bit hardware arithmetic. Weight-activation quantization also increases the throughput of the self-attention layer by reducing the size of the KV-cache, thus decreasing memory movement. However, as Figure 4(b) shows, weight-only quantization fails to improve dense layer throughput since dequantization must be performed before matrix multiplications, yielding calculations still in the floating point format. On the other hand, weight-only quantization fails to quantize the KV-cache, yielding no benefit for self-attention layers. We further quantify the effect of different quantization techniques in Figures 10(a) and 10(b) in §5.

In summary, the low-bit weight-activation quantization is superior to weight-only quantization for enhancing the throughput of the serving scenario because it accelerates both the dense and self-attention layers.

4 Design

Low-bit precision allows the utilization of the underlying hardware efficiently, thus delivering higher throughput. However, it is challenging to achieve high accuracy with a low-bit representation. To quantize LLMs to extremely low-bit precision while keeping accuracy, we incorporate a suite of quantization mechanisms tailored to LLM characteristics. These mechanisms include mixed-precision quantization with reordering, fine-grained group quantization, and dynamic quantization. We demonstrate the accuracy gain thanks to these techniques in Table 4. We also quantize the KV-cache to boost the throughput of Atom. The subsequent subsections delve into the specifics of each mechanism and its advantages, followed by a detailed description of the end-to-end workflow.

4.1 Mixed-precision quantization

Prior works (Dettmers et al., 2022; Lin et al., 2023) observed that a key challenge of LLM quantization is the outlier phenomena in activations. As Figure 5(a) shows, a few channels exhibit large magnitudes that are several orders greater than those of other channels. The large dynamic range of these outliers can substantially increase the quantization error. Therefore, efficiently handling the outliers is crucial in low-bit quantization, and we can quantize outliers and normal values separately to effectively mitigate this challenge.

As Figure 5(b) shows, after we remove the outliers, the remaining channels are much more uniform, which can be effectively expressed by low-bit values. Our results indicate that 8-bit precision representations (such as FP8 (Micikevicius et al., 2022) and INT8) are sufficient to express outliers

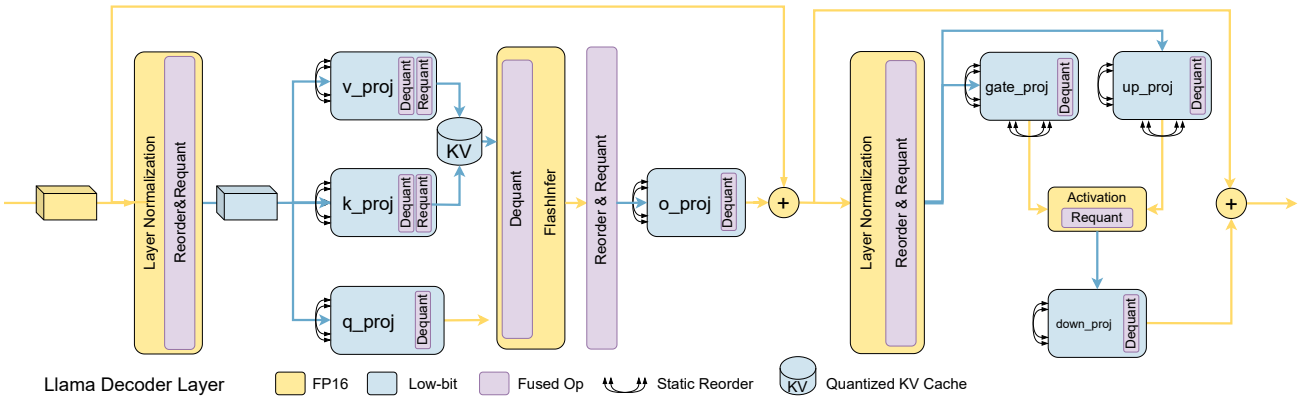

Figure 6. Overview of the Atom workflow on Llama. Atom carefully manages the overhead of quantization operators by fusing them into existing operators. For the compute-bound operators, Atom utilizes efficient low-bit hardware support. For memory-bound self-attention layer, Atom quantizes KV-cache to further enhance the throughput.

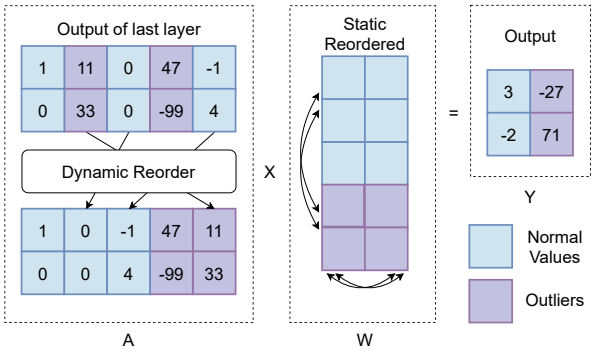

Figure 7. The reorder methodology. We dynamically reorder activation (A) to move the outlier channels to the end of the matrix. The weight matrix (W) is statically reordered to remain aligned with the corresponding activation channels.

(See Table 4). Since INT8 is widely supported by hardware implementations (e.g., Nvidia Tensor cores (Abdelkhalik et al., 2022)), Atom applies INT8 quantization for outliers.

The primary concern with mixed-precision quantization is its irregular memory accesses (Dettmers et al., 2022; Guo et al., 2023), which leads to poor hardware efficiency. To apply mixed-precision quantization while maintaining regular memory access, Atom re-purposes the reordering technique introduced in RPTQ (Yuan et al., 2023), where the objective was to improve inference accuracy. As Figure 7 shows, Atom reorders the scattered outlier channels of activations to the end of the matrix with the goal of enabling the efficient implementation of mixed-precision within a single kernel. Such reorder indices are determined statically using calibration data; thus, reordering of weight matrices is a one-time offline cost. However, the reordering of activation matrices still needs to be performed online, which can be expensive. To mitigate this, Atom fuses the activation matrix reordering into prior operators, which significantly reduces the reordering overhead to 0.5% of runtime.

4.2 Fine-grained group quantization

Even if we quantize outliers and normal values separately, the latter is still challenging to perform accurately due to the limited representation range of 4-bit quantization (Section 5.4). To further enhance accuracy, *group quantization* is widely adopted (Lin et al., 2023; Nagel et al., 2021), which divides the channel into subgroups and performs quantization within each subgroup. For example, a group size of 128 implies that every contiguous sequence of 128 elements in a single channel is treated as a single group. Atom then performs quantization for every group.

Group quantization offers a trade-off between accuracy improvements and dequantization overheads, which has not been investigated by prior work. Atom uses a dedicated high-throughput fusion technique, as shown in Figure 8. Atom first calculates the matrix multiplication of the activation groups with the corresponding weight groups and obtains temporary results using efficient low-bit hardware (Step ①). Atom then adds multiple temporary results together to get the GEMM result. However, since Atom performs quantization for each activation and weight group, each temporary result has different quantization parameters. Therefore, Atom first dequantizes all temporary results to the FP16 representation (Step ②) and then performs addition (Step ③). To manage the overhead, we fuse dequantization and summation into the GEMM kernel so that we are able to perform both operations in place without extra memory movement. We demonstrate the throughput of fused matrix multiplication in §5.3.1.

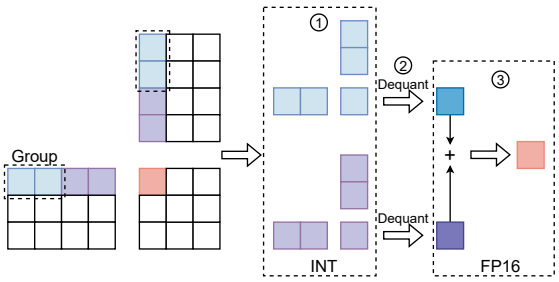

Figure 8. A design overview of fused matrix multiplication. After the multiplication of each group, the result is first dequantized and subsequently accumulated.

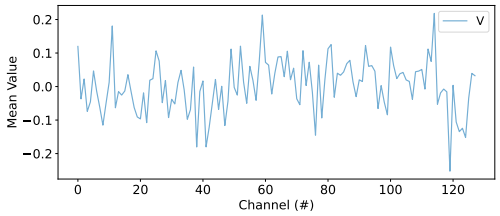

Figure 9. The sampled value of V cache within a single head. Compared with activations shown in Figure 5(a), V cache shows less dynamic range, which is much easier to quantize.

4.3 Dynamic quantization process

Although fine-grained quantization can better preserve the local variations inside each channel of activations, this advantage would diminish if we statically calculated the quantization parameters based on calibration data, as the actual input might have a different local distribution.

Therefore, Atom adopts *dynamic quantization*, tailoring quantization parameters for each activation matrix during inference. To tame the overhead of dynamic quantization, we fuse quantization into the prior operator, akin to the implementation of ZeroQuant (Yao et al., 2022). The run time of the fused dynamic quantization is negligible compared to the dense and self-attention layers, as Figure 3 shows.

However, asymmetric quantization can lead to significant run-time overhead due to considerable additional computation (as discussed in §2). To strike a balance between throughput and accuracy, we choose symmetric quantization with a carefully chosen clip threshold. We also incorporate GPTQ (Frantar et al., 2023) when quantizing the weight matrix since this is purely an offline process and offers an accuracy boost without sacrificing throughput.

4.4 KV-cache quantization

As described in §3, the self-attention layer in the decode stage is highly memory-bound. To mitigate this issue, Atom also applies low-bit quantization to the KV-cache. Atom loads the KV-cache in low-bit precision and directly dequantizes it before performing the FP16 self-attention calculation, because computation is not the bottleneck in this case. On the other hand, since the memory movement of asymmetric and symmetric quantized KV-cache are similar, they perform similarly on memory-bound self-attention layers. Therefore, Atom uses asymmetric quantization as it can provide extra accuracy benefits.

Compared with activation matrices, we argue that the KV-cache is more amenable to quantization. To perform self-attention, the Query vector of the incoming token is multiplied by the K cache. The result is normalized using Softmax, and further multiplied with the V cache to obtain the output. Due to the normalization of Softmax, the quantization error of the K cache has less influence on the output. Furthermore, our profiling in Figure 9 indicates that the V cache exhibits the outlier phenomenon less frequently, rendering it more suitable for quantization. Therefore, Atom directly applies asymmetric low-bit quantization within each attention head and preserves high accuracy as shown in §5.4. We fuse the dequantization with the state-of-the-art self-attention optimization technique, FlashInfer (Ye, 2023), and GPU memory management system, PageAttention (Kwon et al., 2023), to achieve high throughput.

4.5 Implementation of quantization workflow

To demonstrate the feasibility of our design choices, we implement Atom on Llama models (see Figure 6). To leverage the benefit of quantization, we carefully manage the overhead of the additional operators by kernel fusion: Atom fuses quantization operators, including reordering, re-quantization, and dequantization, into existing operators. For the compute-bound dense layer, we use the low-bit calculation to boost throughput. For the memory-bound self-attention layer, we fuse the dequantization with FlashInfer so that we need to load only low-bit integers from the KV-cache to achieve high throughput. We also incorporated PageAttention for efficient usage of memory in order to enable the use of large batch sizes.

5 Evaluation

We now evaluate Atom's accuracy (perplexity, zero-shot) and efficiency (kernel throughput, end-to-end throughput, end-to-end latency) and examine the effectiveness of its different quantization techniques. We begin by reviewing our quantization setup.

5.1 Quantization setup

Atom uses symmetric quantization on weights and activations while using asymmetric quantization on the KV-cache.

Table 1. WikiText2 perplexity on **Llama2** at 7B and 13B.

# Bits	Method	Perplexity ↓ Llama2-7B	Llama2-13B
FP16	-	5.47	4.88
W4A4	SmoothQuant	83.12	26.87
	OmniQuant	14.61	12.3
	Atom	**6.03**	**5.26**
W3A3	SmoothQuant	Inf	Inf
	Atom	15.07	9.29

We evaluate Atom using a group size of 128. To identify outlier channels, we use 128 randomly sampled sentences from WikiText2 (Merity et al., 2016) as calibration data, following prior work (Lee et al., 2023; Shao et al., 2023; Liu et al., 2023a). We then reorder the activations and weights based on the square sum of each activation channel. After reordering, we select 128 channels with the highest square sum values as outliers and keep them in INT8. To apply clipping, we use grid search to find the optimal clipping factors 0.9 and 0.85 for activations and weights, respectively.

For the quantization process, we run Atom on a single RTX 6000 GPU and quantize the model layer-by-layer. For Llama-65B, Atom takes only 4 hours to complete the entire quantization process. In contrast, related work SpQR (Dettmers et al., 2023), takes more than 6 hours while OmniQuant (Shao et al., 2023) takes up to 16 hours, demonstrating the efficiency of our quantization technique.

5.2 Accuracy evaluation

Benchmarks. We evaluate Atom by quantizing Llama (Touvron et al., 2023)[1] models with simulated quantization process following (Xiao et al., 2023). We focus on INT4 and INT3 weight-activation quantization since previous works (Dettmers et al., 2022; Xiao et al., 2023; Shao et al., 2023; Liu et al., 2023a) demonstrated that LLMs can be quantized with negligible accuracy loss using INT8 and INT6 weight-activation quantization. To examine the accuracy, we evaluate Atom on the commonly used metrics, perplexity, and zero-shot accuracy. For perplexity, we evaluate on WikiText2 (Merity et al., 2016), PTB (Marcus et al., 1994), and C4 (Raffel et al., 2020) datasets. For zero-shot accuracy, we use the lm-eval (Gao et al., 2021) and evaluate on PIQA (Bisk et al., 2019), ARC (Clark et al., 2018), BoolQ (Clark et al., 2019), HellaSwag (Zellers et al., 2019), and WinoGrande (Sakaguchi et al., 2019) tasks. We primarily evaluate Atom on Llama-1. Additionally, in order to demonstrate Atom's generalizability, we include perplexity results for Llama-2 at 7B and 13B.

[1]Our Llama-1 and Llama-2 models are downloaded from decapoda-research and meta-llama on HuggingFace.

Baselines. We compare Atom to recently released post-training weight-activation quantization techniques, SmoothQuant (Xiao et al., 2023), OmniQuant (Shao et al., 2023), and QLLM (Liu et al., 2023a). For SmoothQuant, we implement our own version as the official code does not support Llama and only has INT8 quantization. We conducted a grid search on the $alpha$ value defined in the SmoothQuant paper and reported the best numbers for each benchmark. For OmniQuant, we use their pre-trained weights for W4A4 evaluations and train our own results using their official code for W3A3. To obtain W3A3 results for OmniQuant, we use $lr = 1e^{-4}$ and $alpha = 0.75$ after a hyperparameter search. We do not evaluate W3A3 OmniQuant on Llama-30B and Llama-65B due to the large GPU memory requirement of its finetuning process. For QLLM, we report the W4A4 numbers listed in their paper but do not evaluate W3A3 since their code is currently unavailable.

Zero-shot accuracy. Table 2 compares the zero-shot accuracy of six common sense tasks between Atom and our baselines using Llama. Atom significantly outperforms the other weight-activation quantization methods. For W4A4, Atom shows only a 2.3%, 1.7%, 0.4% and 1.4% accuracy loss for Llama at 7B, 13B, 30B and 65B sizes when compared to FP16. At the same time, previous works showed a 9.6% to 24.8% accuracy loss under the same settings. For W3A3, Atom achieves an averaged 9.9% accuracy loss across different Llama sizes, showing significant improvement compared to previous weight-activation quantization methods. This is particularly impressive given that our method requires no computationally heavy finetuning process.

Llama Perplexity. We report Llama perplexity results of Atom and baselines in Table 3. As the table shows, though recent methods such as OmniQuant and QLLM reduce the perplexity of W4A4 to around 10, Atom further reduces the perplexity and achieves a remarkable less than 1 perplexity increase on all three datasets. For W3A3, Atom still strongly maintains the perplexity, with only an average 2.5 perplexity increase for Llama-65B. At the same time, previous works SmoothQuant and OmniQuant do not achieve satisfactory perplexity results (perplexity > 1000). We also notice that Atom achieves lower perplexity increases for larger models.

Llama-2 Perplexity. In addition to the Llama results, we evaluate Atom on Llama-2 and present perplexity results. As Table 1 illustrates, similar to Llama, Atom only increases the perplexity by less than 1 in W4A4, while the baselines have worse perplexity (i.e., greater than 10). For the baseline SmoothQuant at W3A3, we cannot get a real number even after a grid search on $alpha$. However, Atom still maintains a less than 10 perplexity increase for both models at W3A3.

Table 2. **Zero-shot accuracy** of quantized Llama models on six common sense tasks.

Size	#Bits	Method	Zero-shot Accuracy ↑						
			PIQA	ARC-e	ARC-c	BoolQ	HellaSwag	Winogrande	Avg.
7B	FP16	-	77.37	52.53	41.38	73.12	72.99	66.85	64.04
	W4A4	SmoothQuant	63.11	40.03	31.57	58.47	43.38	52.80	48.23
		OmniQuant	66.15	45.20	31.14	63.51	56.44	53.43	52.65
		QLLM	68.77	45.20	31.14	-	57.43	56.67	51.84
		Atom	**76.28**	**52.10**	**38.99**	**69.79**	**69.81**	**63.69**	**61.78**
	W3A3	SmoothQuant	48.69	25.97	28.16	45.26	26.02	49.57	37.28
		OmniQuant	49.78	27.19	27.22	37.86	25.64	49.96	36.28
		Atom	65.56	41.41	30.72	61.77	53.19	55.56	51.37
13B	FP16	-	79.05	59.85	44.62	68.53	76.22	70.09	66.39
	W4A4	SmoothQuant	64.47	41.75	30.89	62.29	46.68	51.70	49.63
		OmniQuant	69.69	47.39	33.10	62.84	58.96	55.80	54.63
		QLLM	71.38	47.60	34.30	-	63.70	59.43	55.28
		Atom	**77.69**	**57.58**	**42.92**	**67.46**	**73.77**	**68.51**	**64.66**
	W3A3	SmoothQuant	47.99	26.30	27.65	46.91	25.65	49.64	37.36
		OmniQuant	50.22	26.77	27.82	37.83	25.77	51.07	36.58
		Atom	70.08	47.94	33.70	63.46	62.93	56.75	55.81
30B	FP16	-	80.20	58.92	45.31	68.38	79.23	72.69	67.46
	W4A4	SmoothQuant	59.30	36.74	28.58	59.97	34.84	49.96	44.90
		OmniQuant	71.21	49.45	34.47	65.33	64.65	59.19	57.38
		QLLM	73.83	50.67	38.40	-	67.91	58.56	57.87
		Atom	**78.73**	**58.92**	**45.82**	**68.47**	**77.40**	**73.09**	**67.07**
	W3A3	SmoothQuant	49.46	27.53	28.16	39.42	26.05	51.38	37.00
		Atom	72.47	49.54	37.80	65.75	66.99	60.14	58.78
65B	FP16	-	80.79	58.71	46.33	82.26	80.71	77.03	70.97
	W4A4	SmoothQuant	60.72	38.80	30.29	57.61	36.81	53.43	46.28
		OmniQuant	71.81	48.02	35.92	73.27	66.81	59.51	59.22
		QLLM	73.56	52.06	39.68	-	70.94	62.90	59.83
		Atom	**80.41**	**58.12**	**45.22**	**82.02**	**79.10**	**72.53**	**69.57**
	W3A3	SmoothQuant	49.56	26.64	29.10	42.97	26.05	51.14	37.58
		Atom	75.84	51.43	41.30	74.07	72.22	64.33	63.20

Table 3. **Perplexity** of quantized Llama models on WikiText2, PTB and C4 dataset.

Size	Bits	Method	Perplexity ↓			Size	Bits	Method	Perplexity ↓		
			WikiText2	PTB	C4				WikiText2	PTB	C4
7B	FP16	-	5.68	8.80	7.08	13B	FP16	-	5.09	8.07	6.61
	W4A4	SmoothQuant	22.62	40.69	31.21		W4A4	SmoothQuant	33.98	73.83	41.53
		OmniQuant	11.59	20.65	14.96			OmniQuant	10.90	18.03	13.78
		QLLM	9.65	-	12.29			QLLM	8.41	-	10.58
		Atom	**6.16**	**9.62**	**7.70**			Atom	**5.46**	**8.60**	**7.03**
	W3A3	SmoothQuant	2.7e4	3.5e4	2.6e4		W3A3	SmoothQuant	1.3e4	1.6e4	1.5e4
		OmniQuant	3.4e3	7.5e3	6.3e3			OmniQuant	7.2e3	1.6e4	1.3e4
		Atom	11.77	20.84	15.43			Atom	8.40	15.84	10.81
30B	FP16	-	4.10	7.30	5.98	65B	FP16	-	3.53	6.91	5.62
	W4A4	SmoothQuant	109.85	142.34	87.06		W4A4	SmoothQuant	88.89	278.76	283.80
		OmniQuant	10.34	14.91	12.49			OmniQuant	9.18	16.18	11.31
		QLLM	8.37	-	11.51			QLLM	6.87	-	8.98
		Atom	**4.54**	**7.69**	**6.35**			Atom	**3.89**	**7.22**	**5.92**
	W3A3	SmoothQuant	1.5e4	1.6e4	1.5e4		W3A3	SmoothQuant	6.6e8	3.7e8	4.4e8
		Atom	6.94	12.12	9.14			Atom	5.89	9.71	7.94

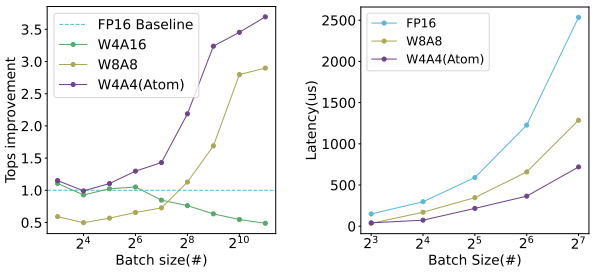

(a) Dense layer (b) Self-attention

Figure 10. Performance evaluation of different quantization approaches on dense layer and self-attention. We evaluate the performance under the Llama-7b config and 1024 sequence length.

5.3 Efficiency evaluation

To demonstrate the throughput of Atom, we conduct experiments measuring both per-kernel and end-to-end throughput. Since the highly efficient INT4 calculation is supported by NVIDIA GPUs, we evaluate Atom with W4A4 quantization on 24GB RTX 4090 with CUDA 12.1.

5.3.1 Kernel evaluation

Matrix multiplication. We evaluate the 4-bit fused GEMM implementation used by Atom in Figure 10(a). We implemented fused GEMM for 8-bit weight-activation quantization (W8A8) and 4-bit weight-only quantization (W4A16) following the existing work (Xiao et al., 2023; Lin et al., 2023) as baselines. For smaller batch sizes, GEMM is memory-bound; thus, weight-only quantization performs effectively. However, as the batch size increases, the efficiency of weight-only quantization diminishes due to expensive FP16 calculations and dequantization overhead. At the same time, 4-bit Atom outperforms all other approaches due to its hardware efficiency. At batch size 512, Atom's matrix-multiplication achieves 3.42× and 1.92× speedup over FP16 and INT8 kernels.

Self-attention. For self-attention, we fuse different quantization approaches into FlashInfer (Ye, 2023), which is optimized FlashAttention (Dao, 2023) for serving. We also integrate PageAttention (Kwon et al., 2023) to increase the memory utilization. We evaluate our implementation and show the results in Figure 10(b). The decrease in bits linearly increases the throughput due to the proportionally reduced memory usage of the KV-cache. At batch size 128, we achieve a 1.79× speedup over INT8 quantization and 3.52× over the FP16 baseline.

5.3.2 End-to-end evaluation

Serving setup. We integrate Atom into an end-to-end evaluation serving framework (Chen, 2023b) to evaluate the throughput in a production scenario. We also integrate W8A8 and W4A16 quantization following previous works (Xiao et al., 2023; Lin et al., 2023) as baselines. To get a representative workload, we use ShareGPT (HuggingFace, 2023) to collect the distribution of prefill and decode request length. We analyze the length of every prompt and the corresponding response. We treat multi-round conversations as requests from multiple users. Specifically, we concatenate all previous prompts and responses and use them as the prompt for the new user request. We vary the batch size from 8 to 256. For each batch size, we produce a request volume that is 20× greater than the batch size itself. All requests are served in a First-Come-First-Serve manner. When a request is finished, we replace it with a new request following the mechanism introduced in Orca (Yu et al., 2022). Due to GPU memory limits, we only show the exact results on small batch sizes. When the memory requirement cannot be satisfied, we also simulate the performance by reusing the KV-caches from a subset of requests while preserving the data access pattern and all calculations.

End-to-end throughput. We show the end-to-end throughput in Figure 11(a). Solid lines represent exact evaluation results, while dashed lines represent estimations due to the lack of memory. Atom significantly outperforms any other quantization on all batch sizes. If we fix the available memory as in Figure 11(c), Atom can achieve larger batch sizes so that its throughput further surpasses all baselines while meeting the latency target. Atom can achieve 7.73× throughput compared to the FP16 baseline and 2.53× throughput compared to INT8 quantization using the same amount of memory. In contrast, weight-only quantization behaves poorly due to the additional dequantization overhead in dense layers under large batch sizes and large memory movement of the KV-cache in the self-attention layer.

End-to-end latency. We also evaluate the latency under different batch sizes. Atom significantly outperforms other quantization methods on every batch size. When we achieve the highest practical performance at batch size 64, our latency is lower than INT8 or FP16 implementations under even smaller batch sizes. Notably, even at batch size 256, our latency is still lower than 100 ms, which has been shown to be the effective reading speed of human eyes by a prior study (Trauzettel-Klosinski et al., 2012).

5.4 Ablation study of quantization techniques

In this section, we examine the accuracy gain or loss of different quantization techniques used in Atom. We first use RTN and adopt per-channel quantization for weights and per-token quantization for activations, which is the standard quantization recipe (Nagel et al., 2021), to quantize the model to W4A4. We then apply other quantization techniques used in Atom, i.e., mixed-precision, quantizing

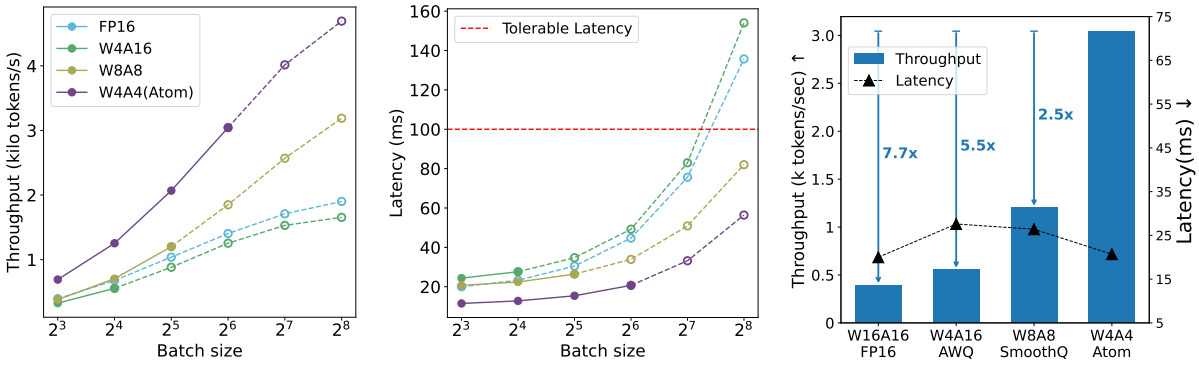

(a) End-to-end throughput (b) Latency per token (c) Throughput and Accuracy comparison given fixed GPU memory

Figure 11. End-to-end evaluation of Atom. Atom surpass all other quantization methods for both throughput and latency. Solid lines are real measurements, dashed lines are estimations due to the limited GPU memory.

Table 4. Ablation study on different quantization techniques used in Atom. The model used in this table is Llama-7B.

Quantization method	**WikiText2 PPL↓**
FP16 baseline	5.68
W4A4 RTN	2382.73
+ Keeping 128 outliers in FP16	11.37 (2371.4↓)
+ Quantizing outliers to INT8	11.39 (0.02↑)
+ Group size 128	6.22 (5.17↓)
+ Clipping	6.13 (0.09↓)
+ GPTQ	6.04 (0.09↓)
+ Quantizing KV-cache to INT4	6.16 (0.12↑)

outliers, group quantization, clipping, GPTQ, and quantizing KV-cache, and examine the perplexity case by case. We present results in Table 4. We see that keeping outlier channels in FP16 can significantly reduce the perplexity for over 2382. Further quantizing outliers into INT8 only results in a very minor 0.02 perplexity increase. These indicate our mixed-precision approach effectively addresses the outlier issue. Besides, fine-grained group quantization brings another major perplexity reduction for 5.17. Furthermore, using clipping and GPTQ lowers perplexity by 0.09 each. After all, quantizing KV-cache results in a small 0.12 perplexity increase, which echoes our finding in §4.4.

In conclusion, mixed-precision and fine-grained group quantization constitute the primary techniques responsible for the significant accuracy enhancement in Atom, while additional optimizations collaboratively contribute to further improvements in Atom's accuracy.

6 Related Work

LLM serving. Various works have studied ways to improve LLM serving throughput. (Pope et al., 2022) investigated the batching effect in scaling up LLM. Orca (Yu et al., 2022) proposed a distributed LLM serving system that uses a fine-grained scheduling policy to improve GPU utilization under various request lengths. vLLM (Kwon et al., 2023) used page tables to manage GPU memory to increase memory utilization, which significantly boosts inference throughput. FlexGen (Sheng et al., 2023) proposed an offload mechanism to support larger batches to achieve high throughput. However, unlike prior work, in this paper, we delve deep into the intersection between quantization and LLM serving.

Weight-only quantization. For large LLMs, weight matrices lead to large memory movement, limiting decode efficiency. Weight-only quantization uses low-bit precision to approximate weight matrices. For instance, GPTQ (Frantar et al., 2023) used 4-bit integers to quantize the weight based on the approximate second-order information. AWQ (Lin et al., 2023) further advanced accuracy by preserving salient weights. SqueezeLLM (Kim et al., 2023) handled outliers through non-uniform quantization and used a sparse format to keep outliers and sensitive weights at high precision. QuiP (Chee et al., 2023) successfully represented weights using 2-bit integers by the adaptive rounding method. Nonetheless, in the LLM serving, the overhead of loading the weight matrix is amortized due to batching. Thus, the dense layer becomes compute-bound, while weight-only quantization fails to use efficient low-bit hardware to deliver ideal throughput.

Weight-activation quantization. Weight-activation quantization quantizes both the weight and activation matrices, which is considered more challenging due to the outlier channels of the activation matrix. LLM.INT8 (Dettmers et al., 2022) used mixed-precision to preserve outlier values in activation matrices. (Xiao et al., 2023; Shao et al., 2023; Yao et al., 2022; Wei et al., 2023) used mathematical equivalent transformations to manage activation outliers. Other

works (Liu et al., 2023a; Wu et al., 2023) used the low-rank matrices to compensate for quantization error. Olive (Guo et al., 2023) used algorithm and architecture co-design to accommodate outliers. RPTQ (Yuan et al., 2023) rearranges the channels to reduce the variance in one quantization cluster, further enhancing the accuracy. However, these works all have low accuracy at low-bit precision. A concurrent work, LLM-FP4 (Liu et al., 2023b), achieves comparable but slightly lower zero-shot accuracy to ours at the 4-bit level. Moreover, this method requires a FP4 format, which does not have any hardware support at the moment. In this work, Atom achieves noteworthy accuracy with a low-bit representation as well as high throughput by utilizing existing efficient hardware units.

7 Conclusion

We presented Atom, a low-bit quantization method that leverages the underlying hardware efficiently to achieve both high accuracy and high throughput for LLM serving. We use mixed-precision quantization with reordering, fine-grained group quantization, dynamic quantization and KV-cache quantization to preserve accuracy while fully exploiting emerging low-bit hardware support. We integrate Atom into an end-to-end serving framework, achieving up to 7.73× throughput enhancement compared to the FP16 baseline as well as maintaining less than 1.6% zero-shot accuracy loss.

References

Abdelkhalik, H., Arafa, Y., Santhi, N., and Badawy, A.-H. Demystifying the nvidia ampere architecture through microbenchmarking and instruction-level analysis, 2022.

Bisk, Y., Zellers, R., Bras, R. L., Gao, J., and Choi, Y. Piqa: Reasoning about physical commonsense in natural language, 2019.

Chee, J., Cai, Y., Kuleshov, V., and Sa, C. D. Quip: 2-bit quantization of large language models with guarantees, 2023.

Chen, L. Dissecting batching effects in gpt inference, May 2023a. URL https://le.qun.ch/en/blog/2023/05/13/transformer-batching/.

Chen, L. Potentials of multitenancy fine-tuned llm serving, Sep 2023b. URL https://le.qun.ch/en/blog/2023/09/11/multi-lora-potentials/.

Clark, C., Lee, K., Chang, M.-W., Kwiatkowski, T., Collins, M., and Toutanova, K. Boolq: Exploring the surprising difficulty of natural yes/no questions, 2019.

Clark, P., Cowhey, I., Etzioni, O., Khot, T., Sabharwal, A., Schoenick, C., and Tafjord, O. Think you have solved question answering? try arc, the ai2 reasoning challenge, 2018.

Dao, T. Flashattention-2: Faster attention with better parallelism and work partitioning, 2023.

Dettmers, T., Lewis, M., Belkada, Y., and Zettlemoyer, L. Llm.int8(): 8-bit matrix multiplication for transformers at scale, 2022.

Dettmers, T., Svirschevski, R., Egiazarian, V., Kuznedelev, D., Frantar, E., Ashkboos, S., Borzunov, A., Hoefler, T., and Alistarh, D. Spqr: A sparse-quantized representation for near-lossless llm weight compression, 2023.

Duarte, F. Number of chatgpt users, Jul 2023. URL https://explodingtopics.com/blog/chatgpt-users.

Elimian, G. Chatgpt costs 700,000 to run daily, openai may go bankrupt in 2024, Aug 2023. URL https://technext24.com/2023/08/14/chatgpt-costs-700000-daily-openai.

Frantar, E., Ashkboos, S., Hoefler, T., and Alistarh, D. Gptq: Accurate post-training quantization for generative pre-trained transformers, 2023.

Gao, L., Tow, J., Biderman, S., Black, S., DiPofi, A., Foster, C., Golding, L., Hsu, J., McDonell, K., Muennighoff, N., Phang, J., Reynolds, L., Tang, E., Thite, A., Wang, B., Wang, K., and Zou, A. A framework for few-shot language model evaluation, September 2021. URL https://doi.org/10.5281/zenodo.5371628.

Guo, C., Tang, J., Hu, W., Leng, J., Zhang, C., Yang, F., Liu, Y., Guo, M., and Zhu, Y. OliVe: Accelerating large language models via hardware-friendly outlier-victim pair quantization. In *Proceedings of the 50th Annual International Symposium on Computer Architecture*. ACM, jun 2023. doi: 10.1145/3579371.3589038. URL https://doi.org/10.1145%2F3579371.3589038.

HuggingFace. Sharegpt vicuna unfiltered, May 2023. URL https://huggingface.co/datasets/anon8231489123/ShareGPT_Vicuna_unfiltered.

Jacob, B., Kligys, S., Chen, B., Zhu, M., Tang, M., Howard, A., Adam, H., and Kalenichenko, D. Quantization and training of neural networks for efficient integer-arithmetic-only inference, 2017.

Kim, S., Hooper, C., Gholami, A., Dong, Z., Li, X., Shen, S., Mahoney, M. W., and Keutzer, K. Squeezellm: Dense-and-sparse quantization, 2023.

Kwon, W., Li, Z., Zhuang, S., Sheng, Y., Zheng, L., Yu, C. H., Gonzalez, J. E., Zhang, H., and Stoica, I. Efficient memory management for large language model serving with pagedattention, 2023.

Lee, C., Jin, J., Kim, T., Kim, H., and Park, E. Owq: Lessons learned from activation outliers for weight quantization in large language models. *ArXiv*, abs/2306.02272, 2023. URL https://api.semanticscholar.org/CorpusID:259076427.

Lin, J., Tang, J., Tang, H., Yang, S., Dang, X., Gan, C., and Han, S. Awq: Activation-aware weight quantization for llm compression and acceleration, 2023.

Liu, J., Gong, R., Wei, X., Dong, Z., Cai, J., and Zhuang, B. Qllm: Accurate and efficient low-bitwidth quantization for large language models, 2023a.

Liu, S., Liu, Z., Huang, X., Dong, P., and Cheng, K. Llm-fp4: 4-bit floating-point quantized transformers, 2023b.

Marcus, M., Kim, G., Marcinkiewicz, M. A., MacIntyre, R., Bies, A., Ferguson, M., Katz, K., and Schasberger, B. The penn treebank: Annotating predicate argument structure. In *Proceedings of the Workshop on Human Language Technology*, HLT '94, pp. 114–119, USA, 1994. Association for Computational Linguistics. ISBN 1558603573. doi: 10.3115/1075812.1075835. URL https://doi.org/10.3115/1075812.1075835.

Merity, S., Xiong, C., Bradbury, J., and Socher, R. Pointer sentinel mixture models, 2016.

Micikevicius, P., Stosic, D., Burgess, N., Cornea, M., Dubey, P., Grisenthwaite, R., Ha, S., Heinecke, A., Judd, P., Kamalu, J., Mellempudi, N., Oberman, S., Shoeybi, M., Siu, M., and Wu, H. Fp8 formats for deep learning, 2022.

Nagel, M., Fournarakis, M., Amjad, R. A., Bondarenko, Y., van Baalen, M., and Blankevoort, T. A white paper on neural network quantization, 2021.

NVIDIA. Nvidia a100 specifications, a. URL https://www.nvidia.com/en-us/data-center/a100/.

NVIDIA. Nvidia tensor core, b. URL https://www.nvidia.com/en-us/data-center/tensor-cores/.

Pope, R., Douglas, S., Chowdhery, A., Devlin, J., Bradbury, J., Levskaya, A., Heek, J., Xiao, K., Agrawal, S., and Dean, J. Efficiently scaling transformer inference. *ArXiv*, abs/2211.05102, 2022. URL https://api.semanticscholar.org/CorpusID:253420623.

Raffel, C., Shazeer, N., Roberts, A., Lee, K., Narang, S., Matena, M., Zhou, Y., Li, W., and Liu, P. J. Exploring the limits of transfer learning with a unified text-to-text transformer. *J. Mach. Learn. Res.*, 21(1), jan 2020. ISSN 1532-4435.

Sakaguchi, K., Bras, R. L., Bhagavatula, C., and Choi, Y. Winogrande: An adversarial winograd schema challenge at scale, 2019.

Shao, W., Chen, M., Zhang, Z., Xu, P., Zhao, L., Li, Z., Zhang, K., Gao, P., Qiao, Y., and Luo, P. Omniquant: Omnidirectionally calibrated quantization for large language models, 2023.

Sheng, Y., Zheng, L., Yuan, B., Li, Z., Ryabinin, M., Fu, D. Y., Xie, Z., Chen, B., Barrett, C. W., Gonzalez, J., Liang, P., Ré, C., Stoica, I., and Zhang, C. High-throughput generative inference of large language models with a single gpu. In *International Conference on Machine Learning*, 2023. URL https://api.semanticscholar.org/CorpusID:257495837.

Touvron, H., Lavril, T., Izacard, G., Martinet, X., Lachaux, M.-A., Lacroix, T., Rozière, B., Goyal, N., Hambro, E., Azhar, F., Rodriguez, A., Joulin, A., Grave, E., and Lample, G. Llama: Open and efficient foundation language models, 2023.

Trauzettel-Klosinski, S., Dietz, K., and the IReST Study Group. Standardized Assessment of Reading Performance: The New International Reading Speed Texts IReST. *Investigative Ophthalmology & Visual Science*, 53(9):5452–5461, 08 2012. ISSN 1552-5783. doi: 10.1167/iovs.11-8284. URL https://doi.org/10.1167/iovs.11-8284.

Wei, X., Zhang, Y., Li, Y., Zhang, X., Gong, R., Guo, J., and Liu, X. Outlier suppression+: Accurate quantization of large language models by equivalent and optimal shifting and scaling, 2023.

Wikipedia contributors. List of qualcomm snapdragon systems on chips — Wikipedia, the free encyclopedia, 2023. URL https://en.wikipedia.org/w/index.php?title=List_of_Qualcomm_Snapdragon_systems_on_chips&oldid=1182026635. [Online; accessed 26-October-2023].

Williams, S., Waterman, A., and Patterson, D. Roofline: an insightful visual performance model for multicore architectures. *Communications of the ACM*, 52(4):65–76, 2009.

Wu, X., Yao, Z., and He, Y. Zeroquant-fp: A leap forward in llms post-training w4a8 quantization using floating-point formats, 2023.

Xiao, G., Lin, J., Seznec, M., Wu, H., Demouth, J., and Han, S. Smoothquant: Accurate and efficient post-training quantization for large language models, 2023.

Yao, Z., Aminabadi, R. Y., Zhang, M., Wu, X., Li, C., and He, Y. Zeroquant: Efficient and affordable post-training quantization for large-scale transformers, 2022.

Ye, Z. FlashInfer: Kernel Library for LLM Serving. https://github.com/flashinfer-ai/flashinfer, 2023.

Yu, G.-I., Jeong, J. S., Kim, G.-W., Kim, S., and Chun, B.-G. Orca: A distributed serving system for Transformer-Based generative models. In *16th USENIX Symposium on Operating Systems Design and Implementation (OSDI 22)*, pp. 521–538, Carlsbad, CA, July 2022. USENIX Association. ISBN 978-1-939133-28-1. URL https://www.usenix.org/conference/osdi22/presentation/yu.

Yuan, Z., Niu, L., Liu, J., Liu, W., Wang, X., Shang, Y., Sun, G., Wu, Q., Wu, J., and Wu, B. Rptq: Reorder-based post-training quantization for large language models, 2023.

Zellers, R., Holtzman, A., Bisk, Y., Farhadi, A., and Choi, Y. Hellaswag: Can a machine really finish your sentence?, 2019.